Journal of Applied Electrochemistry (2007) 37:549–555
DOI 10.1007/s10800-006-9235-7

Electrodeposition of AuCo alloys and multilayers

M. GUAN and E.J. PODLAHA*
Mary A. and Gordon Cain Department of Chemical Engineering, Louisiana State University, South Stadium Road, Baton Rouge, LA 70803, USA
*(*author for correspondence, fax:+1-225-578-1476, e-mail: podlaha@lsu.edu)*

Received 21 February 2006; accepted in revised form 5 September 2006

Key words: cobalt–gold alloys, electrodeposited AuCo, multilayer, non-cyanide electrolyte

Abstract

AuCo alloys and Au/Co multilayers have been fabricated by electrodeposition from non cyanide-containing electrolytes. The effect of pH and citric acid concentration on the deposit composition and current efficiency was investigated. Results showed that a lower citric acid concentration (0.47 M) at pH 6.15 was favored for multilayered Au/Co deposits with disparate compositions in each layer. An increase in the citric acid concentration or pH requires a larger applied current density to achieve the same cobalt concentration, and results in a drop of current efficiency.

1. Introduction

Electrodeposition of soft gold is widely used to fabricate X-ray masks for deep lithography electroforming [1] and in electronic packaging, especially where a high density of input/output (I/O) connections are required [2]. Electrodeposited AuCo alloys (so called hard gold), which has a hardness more than twice elemental Au and better wear resistance [3], has been used extensively in the connector manufacturing industry, such as in multiple-insertion electrical contacts found on printed wiring board contacts or spring contacts [4]. Co and Au multilayers have also been examined as potential giant magnetoresistive materials. Velu et al. [5] measured a CPP GMR of 3% at 4.2 K for Co/Au sandwiches, fabricated by ultrahigh vacuum evaporation. Hutten et al. [6] reported an Au/Co granular structures with GMR of 2.4% at 10 K, fabricated by a melt-spinning technique. However, when depositing on irregular shaped substrates or deep recesses, these methods have intrinsic limitations. In contrast, electrodeposition can fulfill this task cost effectively. Towards this end, Valizadeh et al. [7, 8] electrodeposited Au/Co multilayer thin films and nanowires onto polycarbonate membranes from a cyanide-containing electrolyte.

Cyanide electrolytes pose an environmental threat. The major cyanide releases to water are discharges from metal finishing industries, iron and steel mills, and organic chemical industries. In 1995, United States Environmental Protection Agency (EPA) set a stringent cyanide limit at 0.2 ppm [9]. This rigorous regulation may be economically unfeasible for industry if they continue to use $KAu(CN)_2$ in gold plating. In addition to the environmental issues there are several other shortcomings to the use of $[Au(CN)_2]^-$ which has stimulated this investigation and commercialization of other non-cyanide gold complexes in plating baths. The stability of the gold cyanide complex causes the reduction potential to occur at very negative potentials resulting in the generation of hydrogen, which lowers the plating efficiency [10]. In addition, the alkalinity of gold cyanide baths often leads to the delamination of resist from seed layers [11]. As a consequence, a mildly alkaline or even neutral sulfite-based baths exhibit better resist compatibility [12, 13].

In this study, the electrodeposition of AuCo alloys and Au/Co multilayers from a single, sulfite electrolyte is explored. In the Au–Co sulfite electrolyte, the electrolyte stability, alloy compositions, current efficiencies and partial current densities are examined using a rotating disk electrode. Two types of nanometric materials will be investigated, (i) one-dimensional multilayer structures made of alternating thin layers of different composition, and (ii) two-dimensional wire structures suspended within a three-dimensional matrix.

2. Experimental

A sulfite AuCo electrolyte was developed for thin film and multilayer electrodeposition. The cobalt concentration is kept in great excess compared to gold in order to obtain alloys rich in cobalt, and to make it possible to fabricate multilayers. The electrolyte

Table 1. Composition of AuCo electrolyte

Constituent	g l^{-1}	M
$CoSO_4 \cdot 7H_20$	80	0.29
KOH	120	2.14
Au (Techni® Gold 25E)	0.082	0.00042
$C_6H_8O_4 \cdot H_2O$	Variable	
pH	Variable	
Room temperature		

composition is listed in Table 1. The bath constituents are similar to Ref. [8] with one important change, the cyanide species have been removed. Gold ions were added to the cobalt electrolyte using a commercial gold plating solution containing one troy ounce per gallon of Au(I) ions (Techni Gold 25E, Technic, Inc.). Three different citric acid concentrations (0.47, 0.67 and 0.87 M) and three different pH values (5.15, 6.15, 8.03) were tested.

A copper rotating disk electrode (RDE) with a diameter of 0.6 cm is used as the cathode, at 1600 rpm, where AuCo alloy and Au/Co multilayered thin films are deposited. An anodic alumina oxide (AAO) membrane was used as templates for multilayered nanowire structure plating. The electrode area was 1.767 cm^2, including exposed and unexposed regions. The pore density was 50% reported from the manufacture and an estimate of the active surface area was 0.884 cm^2. A 4×4 cm^2 platinum mesh is used as the anode, affixed to a plastic support. A saturated calomel electrode (SCE) is employed as a reference electrode.

Polarization curves, which relate the current density with the applied potential at steady state, were carried out on a Bas-Zahner IM6 unit with a sweep rate of 2 mV s^{-1}. The potential was corrected for ohmic drop, which was measured by impedance spectroscopy. All potentials presented here are versus SCE with ohmic drop correction. For the Au/Co multilayer thin film electrodeposition, a two-step galvanostatic, square-wave pulse plating method was performed with a PINE potentiostat together with an AMEL function generator.

A Kevex Omicron energy-dispersive X-ray fluorescence (XRF) unit was used to measure the bulk heavy metal composition and thickness of the deposited alloy films. Oxygen is expected to be present on the deposit surface, since Co readily forms a cobalt-oxide in air. However, oxygen present in the bulk would indicate partial reduction of the metal species. Therefore, oxygen in the bulk was examined by X-ray Photoelectron Spectroscope (XPS), Kratos AXIS 165.

Multilayer thin films and nanowires were mounted in epoxy resin and cut to expose the cross-section, and then etched with 0.034 M $K_2Cr_2O_7$, 0.36 M H_2SO_4, and 0.012 M HCl [14]. The nanostructures were confirmed by scanning electron microscopy (Jeol JSM-840A SEM, and Hitachi S-4500II Field Emission SEM with EDAX). The nanometric multilayered microstructures below 50 nm were observed with JEOL 100-CX transmission electron microscopy (TEM), on a holey carbon grid.

3. Results and discussion

Figure 1 shows two polarization curves from an electrolyte with and without gold ions obtained with a copper rotating disk electrode at 1600 rpm. Both electrolytes contained 0.67 M citric acid at a pH of 5.15. The polarization curve shifted to a more noble potential, with addition of the Au sulfite solution. The Au limiting current density occurs in the plateau region of the curve when the potential was between −0.7 and −0.8 V. At more negative potentials, Co is electrodeposited under kinetic control and alloys are obtained in a wide range of composition.

3.1. *Unlayered thin film alloys*

Three different citric acid concentrations were examined in the electrolyte and polarization curves are shown in Figure 2, pH = 5.15. The three solutions contain the same concentration of metal ions, 0.42 mM Au (I) and 0.29 M Co (II), with varying citric acid concentrations:

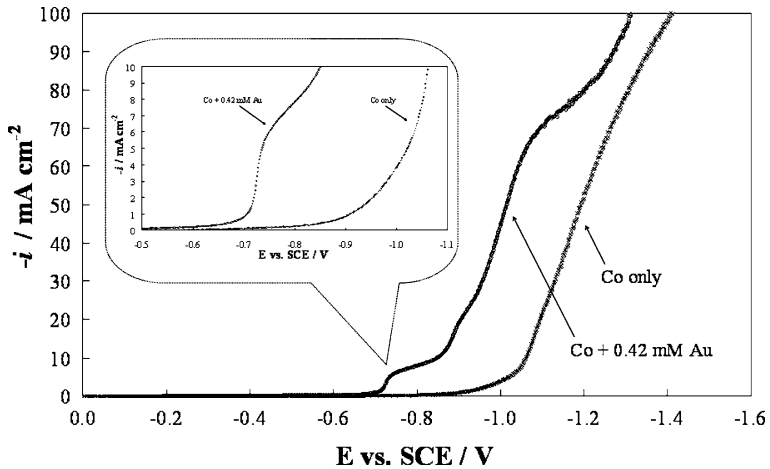

Fig. 1. Polarization curves in Co electrolytes with and without Au addition.

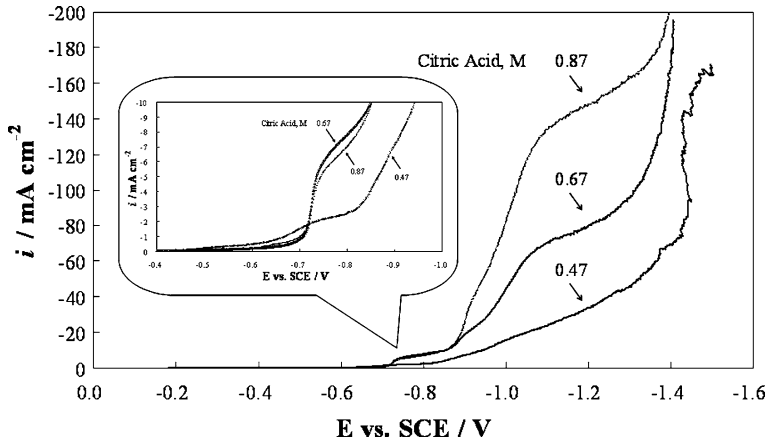

Fig. 2. AuCo polarization curves with different citric acid concentrations.

0.47, 0.67, and 0.87 M, at a rotation rate of 1600 rpm. The inset shows the polarization behavior where primarily Au(I) is reduced. At large overpotentials, the polarization curves increase with an increase in the citric acid concentration. In this region Co and water reduction occurs. The enhanced current density could be attributed to a shift in the Co partial current density due to the formation of Co–citrate complexes or to an increase of the side reaction from reduction of the citric acid. At low current densities (Figure 2, inset), Au electrodeposition and oxygen reduction occur. There is also a change of the total current density with citric acid concentration in this region particularly between 0.47 and 0.67 M.

Figure 3 shows the composition of the resulting alloy. As expected, at low current densities, nearly pure Au is deposited. In contrast, a Co-rich alloy is deposited at high current densities. The citric acid concentration of 0.47 M exhibits the best results for depositing multilayers since the composition is most disparate.

The current efficiency, shown in Figure 4, is affected by the different concentrations of citric acid. The variability is depicted as error bars. At low applied current density the current efficiency is similar for all citric acid electrolyte concentrations, but differs for larger applied current densities (>10 mA cm^{-2}). The current efficiency is higher at 0.47 M citric acid concentration compared to 0.67 and 0.87 M in the region of the Co-alloy plating. All three electrolytes have a similar low current efficiency of 5% at low current density, where Au is plated.

Both the alloy composition and current efficiency were used in the determination of partial current densities of each reactant and to determine the layer thickness used in the pulse plating experiments. The partial current density is important to interpret the changes of the total polarization curves. In determining its value the gold reduction was assumed to occur from a gold species having a $+1$ oxidation state and the cobalt species having a $+2$ oxidation state. The partial current densities of the gold and cobalt reactions are shown in Figure 5(a), and the side reaction partial current density is shown in Figure 5(b). In Figure 5(a), the cobalt partial current density increases with applied potential, as expected for kinetic control. Additional citric acid concentration shifts the Co reaction rate to more

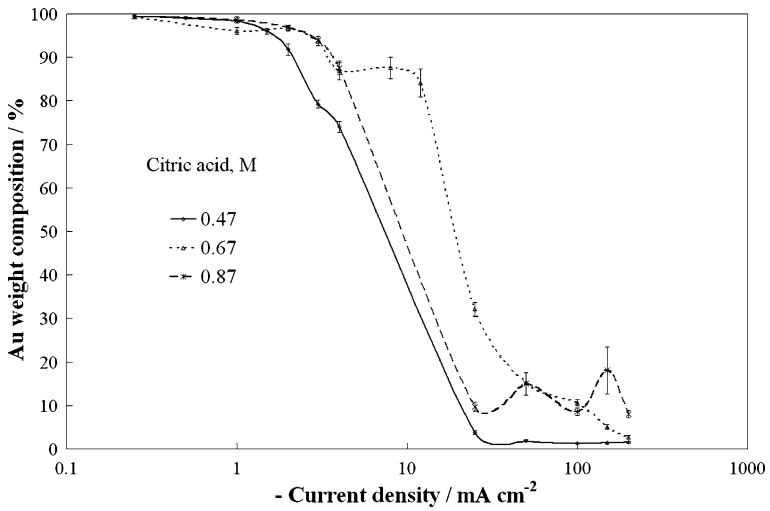

Fig. 3. Au alloy concentration from galvanostatic deposition at different citric acid concentrations.

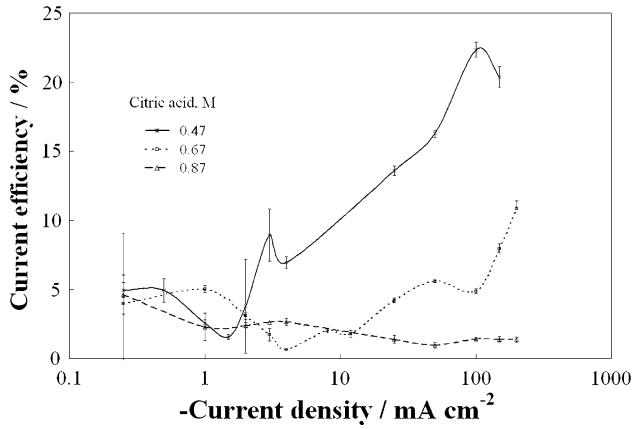

Fig. 4. Current efficiency of the DC plated alloys at different citric acid concentrations.

negative potentials. El Rehim et al. [15] studied the electroplating of cobalt from citrate baths and reported a similar trend due to the change of the Co-ligand species with citrate. The Au reaction rate is not significantly affected by the citric acid concentration. In addition, the partial current density of Au is only a small fraction of the shoulder of the total current density observed in the inset of Figure 1. Furthermore, Figure 5(b) reflects the fact that increasing citric acid concentration increases the side reaction rates, which, consequently, lowers the current efficiency, consistent with Figure 4.

The pH value is expected to impact the bath stability and possibly deposit composition. Five different electrolyte pH values (2.82, 4.04, 5.15, 6.15, 8.03) were examined. Prior to electrodeposition, the solutions were stocked for several days. It was observed that gold precipitation occurred when the pH < 5.0. Therefore three different pH values (5.15, 6.15, 8.03), were examined to find the best electrolyte composition and electrodeposition parameters, to use in the multilayer structure. Figure 6 shows the alloy deposit composition as a function of pH deposited with different applied

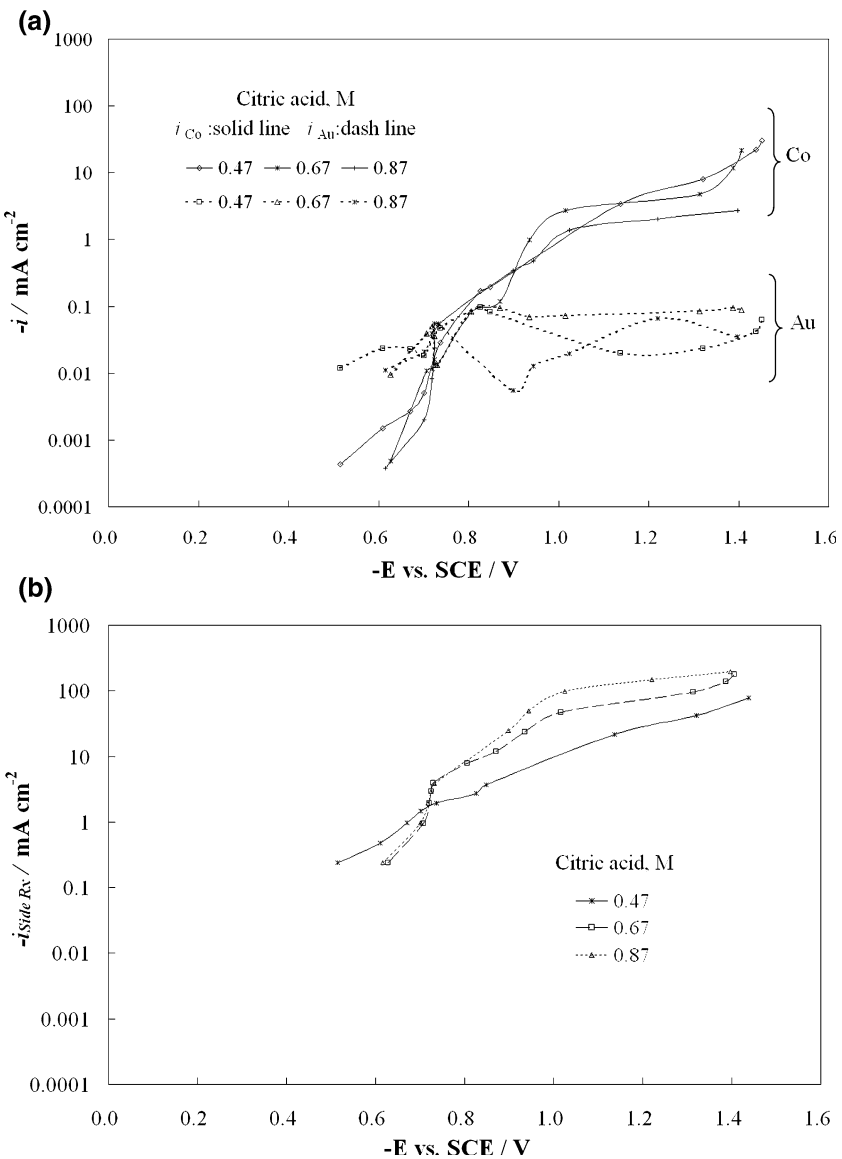

Fig. 5. Partial current densities of (a) Au, Co, and (b) side reaction at different citric acid concentrations.

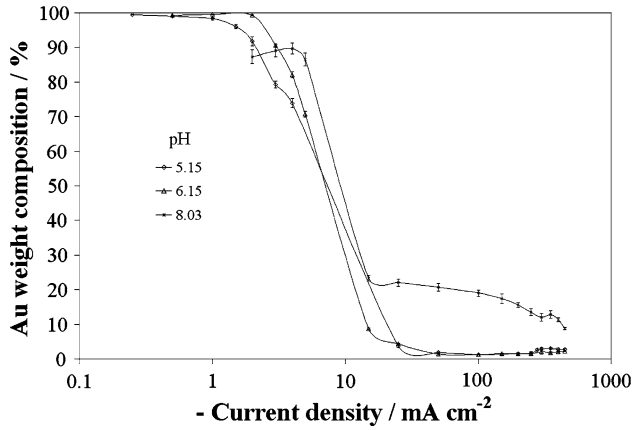

Fig. 6. Au alloy concentration from galvanostatic deposition at different pH values.

current densities at a rotation rate of 1600 rpm. As expected, elemental gold is deposited at low current densities, and a Co-rich alloy is deposited at high current densities. Among the three pH values, the slightly acidic value of 6.15 shows the best results to create the largest difference in deposit composition. The Au content reaches 99.5 wt% when the current density is lower than -1 mA cm^{-2}, and the Co content is higher than 98.7 wt% when the current density is higher than -100 mA cm^{-2}.

Figure 7 shows the current efficiency in the galvanostatic electrodeposition of Au–Co alloys at the three different pH values. The trend is similar to Figure 4. The current efficiency is only 5% at low current densities, and increases approaching a value of 20% at high current densities for the lowest pH value.

Figure 8(a) shows the partial current densities of gold and cobalt reduction and Figure 8(b) shows the partial current densities of the side reactions. In Figure 8(a), as expected, gold exhibits a limiting current at low current densities, and the cobalt partial current density becomes larger with an increase of applied potential, and also reaches a limit. Even though pH does not influence the Au reaction rate, a high pH of 8.03 does shift the Co reaction rate to a more negative potential, resulting in a lower current efficiency. In Figure 8(b), the pH does not significantly alter the side reaction at high currents (or very negative potentials). At low current densities, the low pH of 5.15 has a lower side reaction rate than the higer pH of 8.03 or 6.15. Based on the bath stability and the DC electrodeposited alloy composition, the slightly acid pH of 6.15 was chosen for further study.

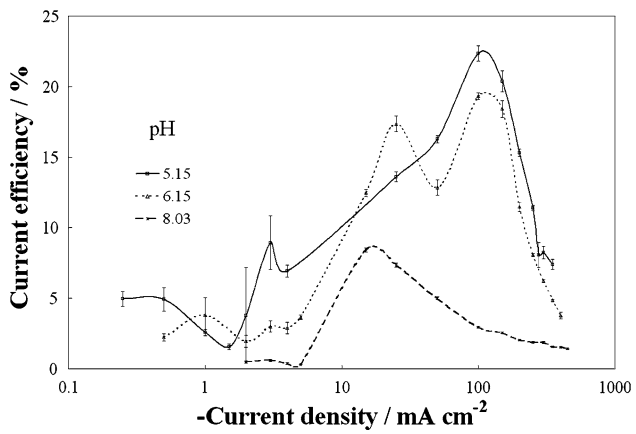

Fig. 7. Current efficiency of the DC plated alloys at different pH values.

3.2. *Co/Au multilayers*

Based on the previous results, galvanostatic, square-wave pulsed plating was carried out with currents of -1 mA cm^{-2} for the Au layer and -100 mA cm^{-2} for the Co layer with variable times. At a low current density elemental gold is deposited, while at a high current density a cobalt rich alloy (98.7% Co) is obtained. XPS analysis was employed to determine if oxygen was present in the film. Figure 9 shows the oxygen content as a function of the etching time of a film containing 5 nm Au layers and 5 nm Co-rich alloy layers, repeated four times. The oxide is only present at the film surface, due to the oxides formed from oxygen in air. In the film depth, no oxygen within the detection error by XPS was detected. This confirms that metallic Au or Co-rich alloy layers are completely reduced and can be plated successfully.

Figure 10 shows an SEM micrograph of Au/Co multilayers with uniform Au/Co layer deposition time, electrodeposited by a galvanostatic, two-step pulse plating. The Au layer was deposited at -1 mA cm^{-2} current density for 5040 s, resulting in a 200 nm thickness. The Co layer was deposited at -100 mA cm^{-2} current density for 90 s, resulting in a 600 nm thickness. The layers look fairly uniform along the direction of growth.

Galvanostatic electroplating was applied to obtain multilayered nanowire structures from an anodic alumina oxide (AAO) membrane with a pore size of 0.02 μm. Au–Co electrolyte composition was the same as in Table 1 but with higher Au concentration of 1.25 mM, due to the longer diffusion path. The conditions for the two-step galvanostatic pulse plating were -0.2 mA cm^{-2} for 180 s for the Au layer and -6 mA cm^{-2} for 24 s for the Co layer. SEM examination shows, in Figure 11(a), the array of multilayered nanowires. A closer inspection with TEM, Figure 11(b) confirms the multilayer structure. The light regions are the Co-rich alloy layer and the dark regions are the Au layer. The layer thickness estimated from the TEM image is 26 nm for Co and 36 nm for Au, which is comparable to the calculated layer size from Faraday's law. The average wire size ranges from 200 to 300 nm, after release from the membrane.

4. Conclusions

In this study, a process of using a non-cyanide single bath to electrodeposit AuCo alloys and multilayers was

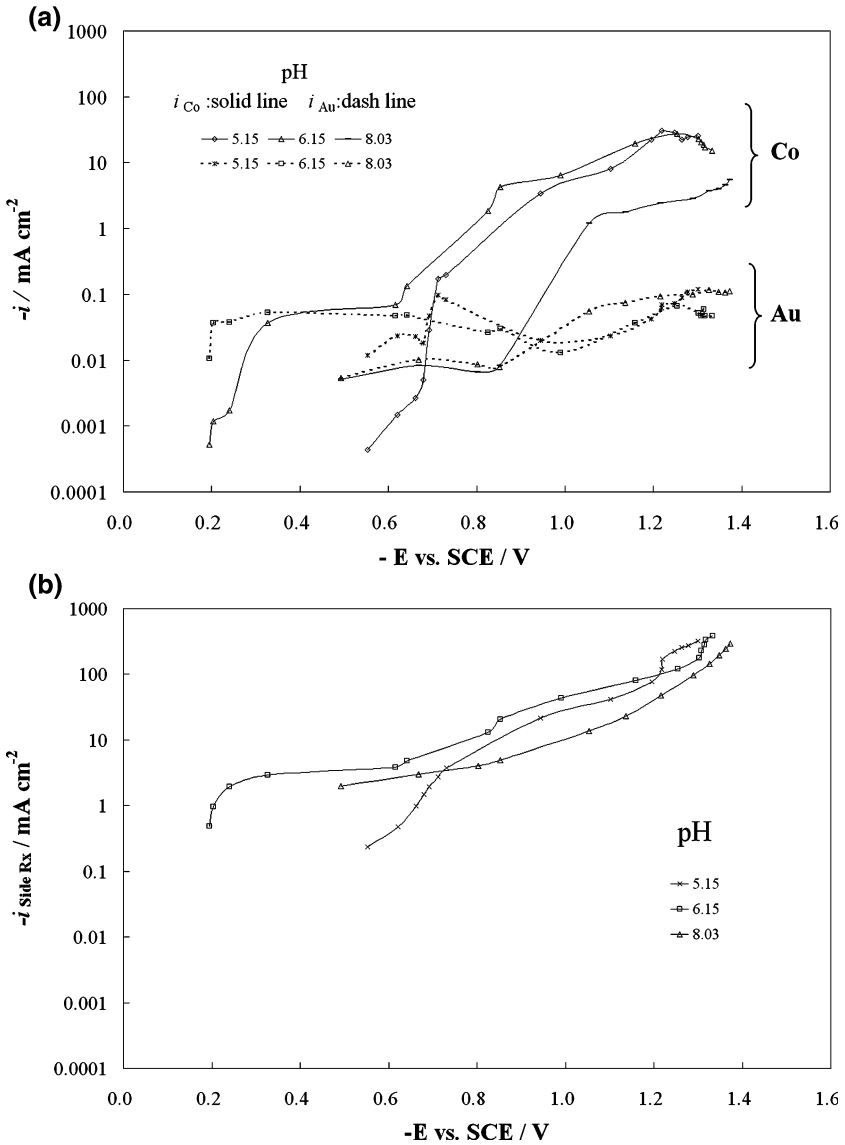

Fig. 8. Partial current densities of (a) Au, Co, and (b) side reaction at different pH values.

characterized. During AuCo deposition, increasing citric acid concentration shifted the Co reaction rate to more negative potentials and increased the side reaction rates, which, consequently, lowers the current efficiency. But increasing citric acid concentration did not significantly

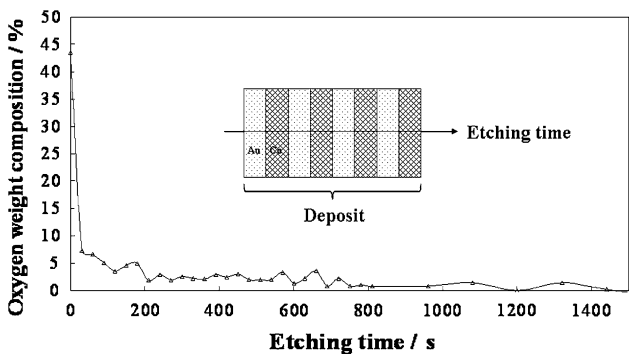

Fig. 9. XPS analysis of Au/Co multilayer films.

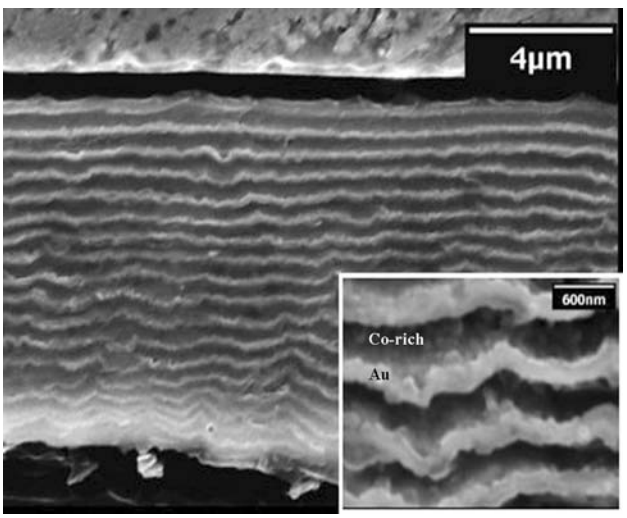

Fig. 10. SEM micrograph of a multilayer with Au/Co layer thickness (Au 200 nm/Co 600 nm) after etching for 5 min.

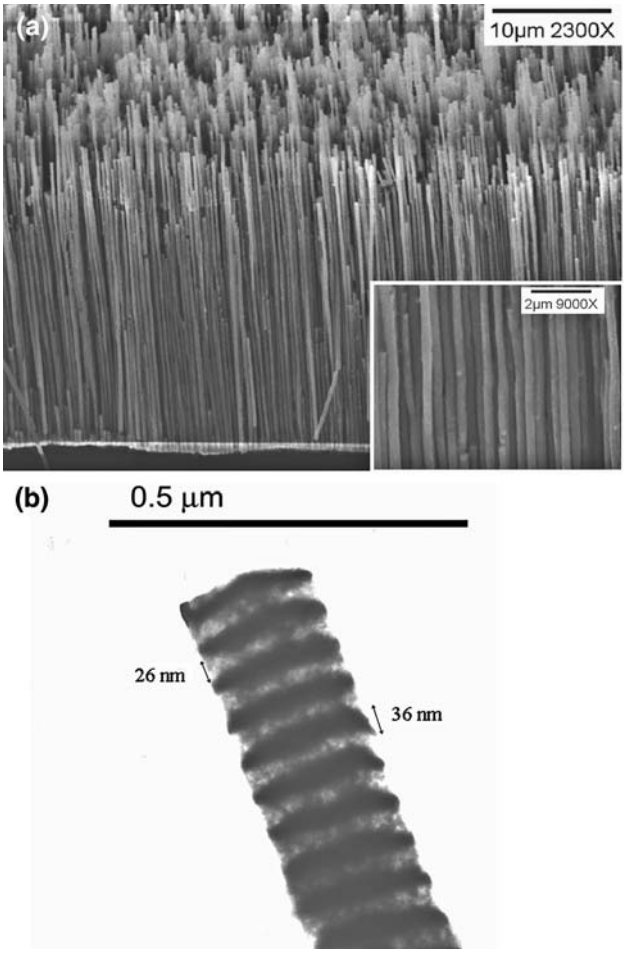

Fig. 11. (a) SEM micrograph of Au/Co multilayer nanowires, and (b) TEM bright field image of a multilayer nanowire.

affect the Au reaction. Even though pH does not influence the Au reaction rate, a higher pH does shift the Co reaction rate to a more negative potential, resulting in a lower current efficiency. The Au content reaches 99.5 wt% when the current density is lower than -1 mA cm^{-2}, and the Co content is higher than 98.7 wt% when the current density is higher than -100 mA cm^{-2}. Au/Co multilayer thin films and nanowires were developed, and confirmed by SEM and TEM.

Acknowledgements

The authors gratefully acknowledge NSF for support of this work under Grant NIRT- NSF (#CTS-0210832) and the Louisiana State University Center for Biomodular Multi-Scale Systems. Also X. Xie and C. Henk are warmly acknowledged for their help in SEM and TEM analyses.

References

1. W. Chu, H.I. Smith, S.A. Rishton, D.P. Kern and M.L. Schattenburg, *J. Vac. Sci. Technol. B* **10** (1992) 118.
2. J. Jasper and D. Shiels, *Eur. Semicond.* **22** (2000) 86.
3. Y. Okinak and M. Hoshino, *Gold Bull.* **31** (1998) 3.
4. P.A. Kohl, *in* M. Schlesinger and M. Paunovic (Eds), 'Modern Electroplating' (J. Wiley & Sons, New York, 4th edn, 2000), 207 pp.
5. E. Velu, C. Dupas, D. Renard, J.P. Renard and J. Seiden, *Phys. Rev. B: Condens. Matter* **37** (1998) 668.
6. A. Hutten, D. Sudfeld, K. Wojczykowski, P. Jutzi and G. Reiss, *J. Magn. Magn. Mater.* **262** (2003) 23.
7. S. Valizadeh, L. Hultman, J.-M. George and P. Leisner, *Funct. Mater.* **12** (2002) 766.
8. S. Valizadeh, E.B. Svedberg and P. Leisner, *J. Appl. Electrochem.* **32** (2002) 97.
9. http://www.epa.gov, (2004).
10. A.M. Sullivan and P.A. Kohl, *J. Electrochem. Soc.* **144** (1997) 1686.
11. J. Traut, J. Wright and J. Williams, *Plat. Surf. Finish* **77** (1990) 49.
12. H. Honma and K. Hagiwara, *Electrochem. Soc.* **142** (1995) 81.
13. K. Kosaki, M. Matsuoka, Y. Seiwa, S. Orisaka, K. Nishitani and M. Otsubo, *in* M. Datta, K. Sheppard and D. Snyder (Eds), 'Electrochemical Microfabrication' (The Electrochemical Society Proceeding Series, Pennington, NJ, 1992), PV 92-3, 317 pp.
14. C. Bonhote and D. Landolt, *Electrochim. Acta* **42** (1997) 2407.
15. S.S.A. El Rehim, S.M.A. El Wahaab, M.A.M. Ibrahim and M.M. Dankeria, *J. Chem. Technol. Biotechnol.* **73** (1998) 369.